Identification of Thermal Parameters of a Solar Photovoltaic Panel in Three-Dimensional using Finite Element Approach

Naima Boulfaf*‡, Jamal Chaoufi*

* Laboratory of Electronics, Signal Processing and Physical Modeling, Department of Physics, Faculty of Sciences, IBN ZOHR University, 80000, Agadir, Morocco
(naimaboulfaf@gmail.com, j.chaoufi@uiz.ac.ma)

‡ Corresponding Author; Naima Boulfaf, Ibn Zohr University, 80000 Agadir, Morocco, Tel.: +212693975608,

naima.boulfaf@edu.uiz.ac.ma

Received: 24.10.2016 Accepted: 10.12.2016

Abstract- The focus of this study is to develop a computer program that simulates the thermal performance of a photovoltaic (PV) panel. A detailed thermal model of a solar PV panel in three-dimensional using finite element approaches is established to determine the thermal parameters. The PV cell, glass, and tedlar temperatures are predicted. The influence of air velocity, solar flux, and ambient temperature are investigated. Simulation results indicate that whatever the value of air temperature and solar irradiance, the solar cell component has a high temperature. The obtained results also show that the PV panel temperature increases when the solar flux and the ambient temperature increases, consequently, the panel efficiency decreases. Finally, it is found that the highest value of wind speed causes the cooling of solar cells leading to the decrease of the PV panel temperature.

Keywords- Finite element approach, Photovoltaic, Thermal model, Temperature.

1. Introduction

Solar energy represents an immense and renewable resource just waiting to be used more extensively. The photovoltaic industry is expanding rapidly associated with the intensive research to increase the efficiencies of the photovoltaic conversion and reduces production costs in order to make this energy source increasingly competitive. The photovoltaic collector converts sunlight directly into electrical energy. The performance of photovoltaic panels depends directly on the PV cell temperature. Several theoretical and experimental works have been done to increase the thermal and electrical performance of such collectors.

A dynamic thermal model for predicting the PV module temperature under different atmospheric conditions has been developed [1,2]. The previous study in modeling the operating temperature of solar cells has focused on obtaining correlations expressing the PV temperature as a function of solar irradiance, ambient temperature, and wind speed [3-14]. The performance and thermal behavior of PV modules have been discussed in the literature [15-20].

Several three-dimensional thermal models have been carried out to simulate the thermal characteristics and performance of PV modules [21-23]. Based on this literature review, we have proposed in this study a detailed systematic approach predicting the thermal behavior of PV panel; this approximation consists of dividing the geometry and approximating the temperatures sought. This step makes it possible to write the problem to solve in a divided form, which is very appropriate for a computer numerical solution. This model will be used to study the temperature distribution in the various components of the system. Modeling PV module allows the optimization of this system for better performance which means better exploitation of solar energy.

1. Methodology

The role of the photovoltaic panel is to convert solar radiation into electrical energy. The studied PV module consists of three material layers: the first is glass layer that is the face exposed to the incident radiation, the second layer containing the photovoltaic cells that convert the absorbed solar radiation into electrical energy and the third is tedlar back sheet that is the protective layer. Fig. 1 shows the cross-sectional view of this panel. The temperature distribution is evaluated using the function $T(x,y,z,t)$ named the temperature function. The initial temperature distribution is known, we will denote it $T_0(x,y,z) = T_a$. The photovoltaic panel receives the solar flux G and its lateral and transversal faces are assumed to be thermally insulated.

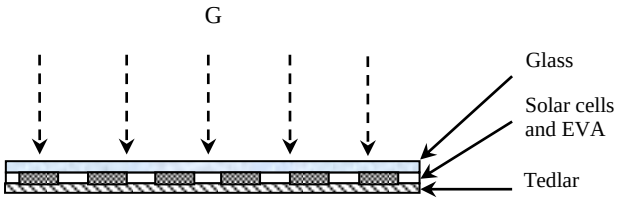

Fig. 1. Diagram considered for studied PV module.

2.1. Thermal Analysis

The theoretical models are used to predict the thermal production of photovoltaic panels. These models are based on the distribution of heat flow in the different layers of the PV panel. Modeling is performed in steady state by imposing particular hypothesis:

∞ All materials constituting the PV module are supposed to be isotropic and independent of temperature,
∞ The wind direction is parallel to the surface of the glass,
∞ $h_{front\ surface} = \left(h_{back\ surface}/2\right)$ [24].

2.1.1. Strong Form

The objective is to predict the temperatures in each layer of PV panel, for that we use the principle of conservation of energy for each system component that can be presented by the following heat transfer equation [25,26]:

$$\rho c \frac{\partial T}{\partial t} = div\left(\bar{\bar{\lambda}}\,\overrightarrow{grad}T\right) \tag{1}$$

Where the thermal conductivity tensor $\bar{\bar{\lambda}}$ of isotropic material has as matrix representation in orthonormal basis $\{x,y,z\}$:

$$[\lambda] = \lambda\begin{bmatrix}1 & 0 & 0\\ 0 & 1 & 0\\ 0 & 0 & 1\end{bmatrix}$$

Solving a thermal problem consists in searching the temperature field $T(x,y,z)$ at any point in PV panel such as:

$$\rho c \frac{\partial T}{\partial t} - div\left(\bar{\bar{\lambda}}\,\overrightarrow{grad}T\right) = 0$$

In order to calculate the temperature field of PV panel, we must write the thermal balance for each layer, taking account of energy loss by conduction, convection, and radiation. The layers for which the temperature is evaluated are glass, solar cells, and tedlar. The boundary and initial conditions for each component of PV panel can be written as:

– **Initial condition**

$$T_0(x,y,z) = T_a$$

– **Boundary conditions**

- *For glass*

$$-\lambda_g \overrightarrow{grad}T_g.\vec{n} = \alpha_g G - h_{g-a}\left(T_g - T_a\right) - \sigma\varepsilon_g\left(T_g^4 - T_{sky}^4\right) \tag{2a}$$

$$-\lambda_g \overrightarrow{grad}T_g.\vec{n} = \alpha_g \tau_g G \tag{2b}$$

- *For solar cells*

$$-\lambda_c \overrightarrow{grad}T_c.\vec{n} = \alpha_c \tau_g G \tag{3a}$$

$$\varphi = \eta_{ref}\left[1 - \beta_0\left(T_c - T_{ref}\right)\right]G \tag{3b}$$

- *For tedlar*

$$-\lambda_{ted}\overrightarrow{grad}T_{ted}.\vec{n} = -h_{ted-a}(T_{ted} - T_a) - \sigma\varepsilon_{ted}\left(T_{ted}^4 - T_{ground}^4\right) \tag{4}$$

2.1.2. Weak Form

The local formulation represented by Eqs. (2), (3) and (4) could not be used directly to solve the Eq. (1) using the finite element method. We, therefore, formulate the problem in a global manner that is easy to solve with finite element method. Under these conditions, the variational formulation often called weak form is written in each layer as follows [26]:

- *Glass*

$$\int_{V_g} \rho_g c_g T_g^* \left(\frac{\partial T_g}{\partial t}\right) dV - \int_{S_{g2}} T_g^*\,\alpha_g \tau_g G dS - \int_{S_{g1}} T_g^*\left(\alpha_g G - h_{g-a}\left(T_g - T_a\right) - \sigma\varepsilon_g\left(T_g^4 - T_{sky}^4\right)\right) dS + \int_V \overrightarrow{grad}T_g^*\left(\bar{\bar{\lambda}}_g\,\overrightarrow{grad}T_g\right) dV = 0 \tag{5}$$

- *Solar cells*

$$\int_{V_c} \rho_c c_c T_c^* \left(\frac{\partial T_c}{\partial t}\right) dV - \int_{S_{c1}} T_c^* \left(\alpha_c \tau_g G\right) dS + \int_{V_c} \overrightarrow{grad} T_c^* \left(\bar{\bar{\lambda}}_c \overrightarrow{grad} T_c\right) dV + \int_{V_c} T_c^* (\eta_{ref} \beta_0 T_c G) dV - \int_{V_c} T_c^* \eta_{ref} G\left[1 + \beta_0 T_{ref}\right] dV = 0 \quad (6)$$

- *Tedlar*

$$\int_{V_{ted}} \rho_{ted} c_{ted} T_{ted}^* \left(\frac{\partial T_{ted}}{\partial t}\right) dV + \int_{V_{ted}} \overrightarrow{grad} T_{ted}^* \left(\bar{\bar{\lambda}}_{ted} \overrightarrow{grad} T_{ted}\right) dV - \int_{S_{ted2}} T_{ted}^* \left(-h_{ted-a}(T_{ted} - T_a) - \sigma \varepsilon_{ted}\left(T_{ted}^4 - T_{ground}^4\right)\right) dS = 0 \quad (7)$$

2.1.3. Finite Element Treatment

The finite element approximation is based on the weak form described in Eqs. (5), (6), and (7). It consists of dividing the geometry of study (PV panel) into sub-domains named finite elements connected at nodes [26]. The geometry of these elements is eight-node hexahedral.

2.1.3.1. Element Quantities

After calculation and simplification, Eqs. (5), (6), and (7) of the corresponding element reduces to the ordinary differential equation [26].

$$[c^e]\{\dot{T}^e\} + [k^e]\{T^e\} = \{f^e\} \quad (8)$$

where $[c^e]$, $\{T^e\}$, $[k^e]$ and $\{f^e\}$ represent heat capacity matrix, nodal vector temperature, thermal conductivity matrix and vector of nodal flow of the element, respectively. For each component we have:

- *In glass*

$$\left[c_g^e\right] = \rho_g c_g \int_{V_g^e} [N^e]^T [N^e] dV^e \quad (9a)$$

$$\left[k_g^e\right] = \int_{V_g^e} [B^e]^T \left[\lambda_g\right] [B^e] dV^e + \int_{S_{g1}^e} [N^e]^T h_{g-a} [N^e] dS^e \quad (9b)$$

$$\left\{f_g^e\right\} = \int_{S_{g1}^e} [N^e]^T \left(\alpha_g G + h_{g-a} T_a - \sigma \varepsilon_g \left(T_g^4 - T_{sky}^4\right)\right) dS^e + \int_{S_{g2}^e} [N^e]^T \alpha_g \tau_g G dS^e \quad (9c)$$

- *In solar cells*

$$[c_c^e] = \rho_c c_c \int_{V_c^e} [N^e]^T [N^e] dV^e \quad (10a)$$

$$[k_c^e] = \int_{V_c^e} [B^e]^T [\lambda_c] [B^e] dV^e + G \eta_{ref} \beta_0 \int_{V_c^e} [N^e]^T [N^e] dV^e \quad (10b)$$

$$\{f_c^e\} = \alpha_c \tau_g G \int_{S_{c1}^e} [N^e]^T dS^e + \eta_{ref} G\left[1 + \beta_0 T_{ref}\right] \int_{V_{c1}^e} [N^e]^T dV^e \quad (10c)$$

- *In tedlar*

$$[c_{ted}^e] = \rho_{ted} c_{ted} \int_{V_{ted}^e} [N^e]^T [N^e] dV^e \quad (11a)$$

$$[k_{ted}^e] = \int_{V_{ted}^e} [B^e]^T [\lambda_{ted}] [B^e] dV^e + \int_{S_{ted2}^e} [N^e]^T h_{ted-a} [N^e] dS^e \quad (11b)$$

$$\{f_{ted}^e\} = \int_{S_{ted2}^e} [N^e]^T \left(h_{ted-a} T_a - \sigma \varepsilon_{ted}\left(T_{ted}^4 - T_{ground}^4\right)\right) dS^e \quad (11c)$$

2.1.3.2. Assembly and Global Quantities

To construct the equation system to solve we must be using the assembly operation which consists of transforming the elementary quantities in global quantities.

i. Elementary assembly

At each layer the ordinary differential system obtained can be written as [26]:

$$\left[c_{layer}\right]\{\dot{T}_{layer}\} + \left[k_{layer}\right]\{T_{layer}\} = \{f_{layer}\} \quad (12)$$

c, k and f are given as follows:

$$[c_{layer}] = \sum_{e=1}^{e=n_t} ([A^e]^T [c^e][A^e]) \quad (13a)$$

$$[k_{layer}] = \sum_{e=1}^{e=n_t} ([A^e]^T [k^e][A^e]) \quad (13b)$$

$$\{f_{layer}\} = \sum_{e=1}^{e=n_t} [A^e]^T \{f^e\} \quad (13c)$$

ii. Global assembly

The assembly of previous matrices (matrices at layers) leads to the following equation [26]:

$$[C]\{\dot{T}\} + [K]\{T\} = \{F\} \quad (14)$$

The capacity and conductivity global matrices $[C]$ and $[K]$, as well as the load vector $\{F\}$ are obtained by assembly operations:

$$[C] = \sum_{layer=1}^{3} [P_{layer}]^T [c_{layer}] [P_{layer}] \quad (15a)$$

$$[K] = \sum_{layer=1}^{3} [P_{layer}]^T [k_{layer}] [P_{layer}] \quad (15b)$$

$$\{F\} = \sum_{layer=1}^{3} [P_{layer}]^T \{f_{layer}\} \quad (15c)$$

Finally, the numerical resolution of the previous equation (Eq. (14)) allows the determination of temperature evolution in the PV module.

With the initial conditions: $\{T_0\} = \begin{Bmatrix} T_1(0) \\ T_2(0) \\ \vdots \\ T_N(0) \end{Bmatrix}$ (16)

2.1.4. Numerical Resolution

We can calculate the convective heat transfer coefficient using the following relation [15]:

$$h = 5.82 + 4.07v \quad (17)$$

We have studied the temperature distribution in the different layer of the photovoltaic module. We have established by numerical simulation the thermal behavior of this module as well as the temperature cartography. The studied geometry is a parallelepiped consisting of three domains: glass, solar cell, and tedlar. The values of the thermal parameters and optical proprieties of all layers are shown in Table 1.

Table 1. Parameter values of PV module.

parameter	Glass	Silicon	Tedlar
Thermal conductivity	1.8	148	0.2
Density	3000	2330	1200
Specific heat Capacity	500	677	1250
Absorbtivity	0.04	0.9	0.128
Reflectivity	0.04	0.08	0.86
Transmissivity	0.92	0.02	0.012
Emissivity	0.85	-	0.9

2.1.4.1. Meshes

In calculation and simulation did previously, we have adopted the mesh of Fig. 2 in which we have chosen to generate a structured mesh with the hexahedral elements. The thicknesses are very fine, for this we hardly differentiate the different layers.

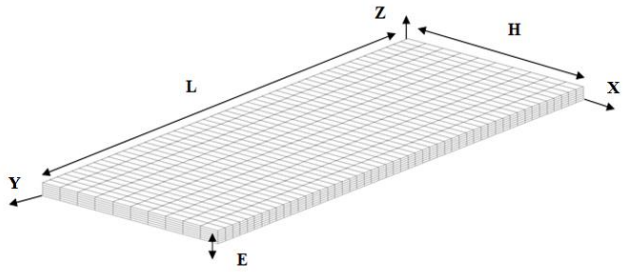

Fig. 2. Finite element mesh of a photovoltaic panel.

2. Results and Discussion

To determine the temperature profile of PV module, Eqs. (14) and (16) have been used for given parameters shown in Table 1. Regular conditions considered are solar flux $G = 1000\ W/m^2$ and ambient temperature $T_a = 25\ °C$. Fig. 3 shows the temperature profile of PV panel and Fig. 4 represents the distribution of temperature according to the thickness of the panel. We observed that the solar cell temperature equals to 64 °C is significantly higher than the glass and the back surface (tedlar) temperatures. Due to layers being very fine the temperature difference between the three layers is not more than 1 °C. It has also observed in each figure that the variation of tedlar temperature is more evident than glass due to thermal heat produced by solar cells and low thermal conductivity of tedlar material.

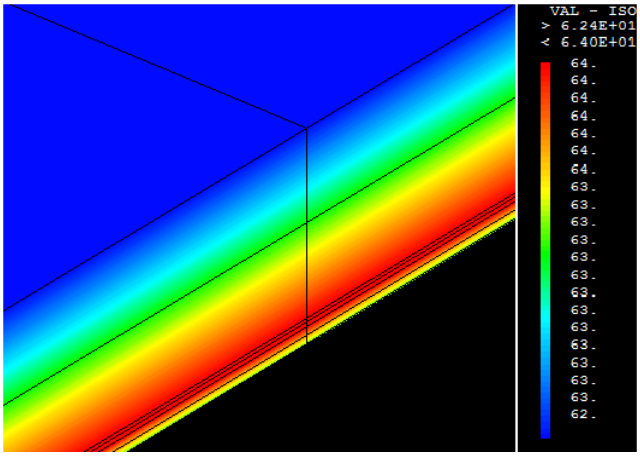

Fig. 3. The three-dimensional temperature profile of PV module.

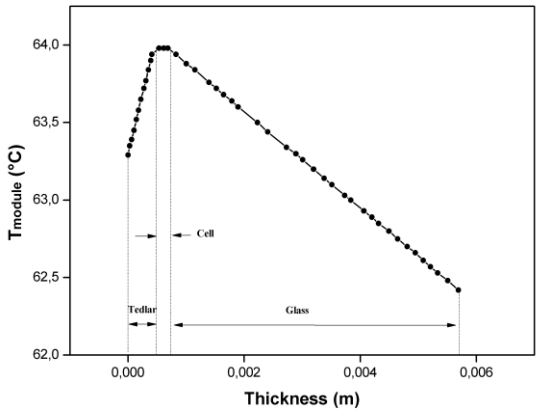

Fig. 4. Temperature evolutions in the PV module according to the thickness.

Solar radiation is the most important factor influencing the functioning of the solar system. Therefore, it would be interesting to study its effect on the system characteristics. To see the influences of solar intensity variations in the PV panel temperatures, the developed model was used, and the results are shown in Fig. 5a and b. It has been found from Fig. 5a that when solar irradiance increases from $G = 200\,W/m^2$ to $G = 1000\,W/m^2$, the PV cell temperature also increases from $T_c = 32.88\,°C$ to $T_c = 63.98\,°C$ as a result of absorbed solar radiations which are not converted into electricity. From Fig. 5b it is evident that the behavior of PV cells is greater under lower ambient temperature. Therefore, high solar intensity leads to decrease electrical efficiency and increase the thermal efficiency of PV module indirectly.

Fig. 6 shows the effect of wind speed variation on PV cell temperature. It is observed that the increase in wind speed from $v = 0\,m/s$ to $v = 10\,m/s$ will decrease PV cell temperature from $T_c = 90.68\,°C$ to $T_c = 33.9\,°C$ because the temperature is related to the wind speed by the convective heat transfer coefficient (Eq. (17)). The same coefficient causes another increase in heat losses that causing a decrease in the PV panel performance. It is also observed that there is a significant decrease in PV cell temperature when the air velocity is lower ($v = 0$ to $v = 1\,m/s$). Consequently, high air velocity leads to best PV panel performance.

Another important environmental parameter that affects PV performance is the temperature ambient. Fig. 7a and b show ambient temperature effects on the PV cell temperature. From Fig. 7a it can be observed that increases in room temperature from $T_a = 0\,°C$ to $T_a = 50\,°C$ will increase PV cell temperature from $T_c = 39.05\,°C$ to $T_c = 89.04\,°C$. Fig. 7b indicates that the increase in PV cell temperature is more obvious when the solar intensity and ambient temperature are higher.

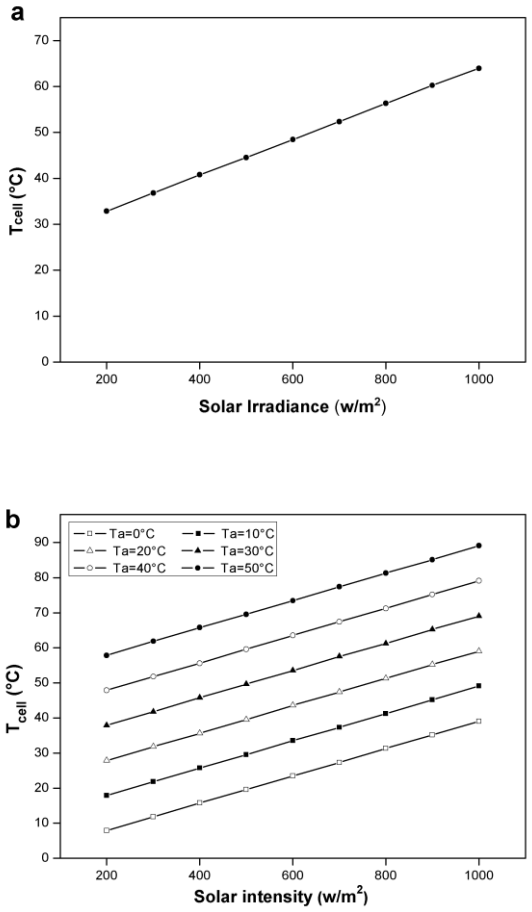

Fig. 5. (a) PV cell temperature variation with solar intensity (Ta = 25 °C). (b) PV cell temperature variation with solar intensity for different ambient temperatures.

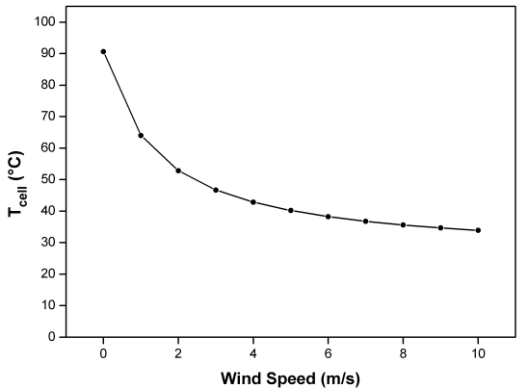

Fig. 6. PV panel performance variations with wind speed.

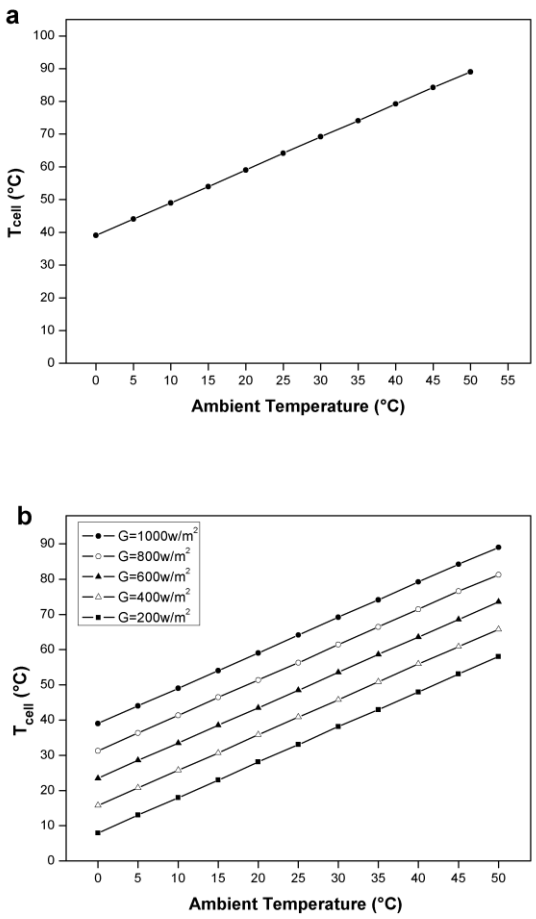

Fig. 7. (a) PV cell temperature variation with ambient temperature (G = 1000 W/m^2). (b) PV cell temperature variation with ambient temperature for different solar intensity.

3. Conclusion

This work summarized a detailed 3D thermal study of a photovoltaic module. We have studied the temperature distribution of different layers of a photovoltaic panel. We established by numerical simulation the thermal behavior of PV panel as well as temperature cartography according to initial and boundary conditions that we mentioned above. The results obtained show that the PV cells temperature increases when the intensity and the ambient temperature increases, also the back surface (tedlar) has a higher temperature than the front surface (glass). Increasing wind speed causes a cooling effect on the exterior glass surface, causing a significant reduction in the PV cell temperature. Therefore, low ambient temperature and high wind speed are two interesting parameters offering the best performance of photovoltaic panels. Finally, this numerical simulation can help the industrial to better control and understand this type of system. With the created program we can put the characteristics that we want to see what material offers the optimum temperature.

References

[1] Jones, A.D. & Underwood, C.P, "A thermal model for photovoltaic systems", Solar Energy, 70, pp. 349–359, 2001.

[2] Lobera, D. T. & Valkealahti, S., "Dynamic thermal model of solar PV systems under varying climatic conditions", Solar Energy, 93, pp. 183–194, 2013.

[3] Skoplaki, E., Boudouvis, A.G.& Palyvos, J.A., "A simple correlation for the operating temperature of photovoltaic modules of arbitrary mounting", Solar Energy Materials & Solar Cells, 92, pp. 1393–1402, 2008.

[4] Schott, T., "Operation temperatures of PV modules", In: Proceedings of the 6th EC Photovoltaic Solar Energy Conference, pp. 392–396, London, 1985.

[5] Servant, J.M., "Calculation of the cell temperature for photovoltaic modules from climatic data", In: Proceedings of the 9th Biennial Congress of ISES – Intersol 85, 370, Montreal, Canada, 1985.

[6] Malik, A.Q. & Damit, S.J.B.H., "Outdoor testing of single crystal silicon solar cells", Renewable Energy, 28, pp. 1433–1445, 2003.

[7] Nordmann T. & Clavadetscher L., "Understanding temperature effects on PV system performance", Proceedings of the third world conference on photovoltaic energy conversion, pp. 2243–2246, Osaka, Japan, 2003.

[8] Krauter, S.C.W., "Development of an integrated solar home system", Solar Energy Materials & Solar Cells, 82, pp. 119–130, 2004.

[9] Franghiadakis, Y. & Tzanetakis, P., "Explicit empirical relation for the monthly average cell-temperature performance ratio of photovoltaic arrays", Progress in Photovoltaics Research and Applications, 14, pp. 541–551, 2006.

[10] Chenni, R., Makhlouf, M., Kerbache, T. & Bouzid, A., "A detailed modelling method for photovoltaic cells", Energy, 32, pp. 1724–1730, 2007.

[11] Mattiei, M., Notton, G., Cristofari, C., Muselli, M. & Poggi, P., "Calculation of the polycrystalline PV module temperature using a simple method of energy balance", Renewable Energy, 31, pp. 553–567, 2006.

[12] Durisch, W., Bitnar, B., Mayor, J.-C., Kiess, H., Lam, K.-H. & Close, J., "Efficiency model for photovoltaic modules and demonstration of its application to energy yield estimation", Solar Energy Materials & Solar Cells, 91, pp. 79–84, 2007.

[13] Topi, M., Brecl, K. & Sites, J., "Effective efficiency of PV modules under field conditions", Progress in Photovoltaics Research and Applications, 15, pp. 19–26, 2007.

[14] Skoplaki, E. & Palyvos, J.A., "On the temperature dependence of photovoltaic module electrical performance: a review of efficiency/power correlations", Solar Energy, 83, pp. 614–624, 2009.

[15] Notton, G., Cristofari, C., Mattei, M. & Poggi, P., "Modelling of a double-glass photovoltaic module using finite differences", Applied Thermal Engineering, 25, pp. 2854-2877, 2005.

[16] Armstrong, S. & Hurley, W.G., "A thermal model for photovoltaic panels under varying atmospheric conditions", Applied Thermal Engineering, 30, pp. 1488–1495, 2010.

[17] Park, K. E., Kang, G. H., Kim, H. I., Yu, G. J. & Kim, J. T., "Analysis of thermal and electrical performance of semi-transparent photovoltaic (PV) module", Energy, 35, pp. 2681–2687, 2010.

[18] Kim, J. P., Lim, H., Song, J. H., Chang, Y. J. & Jeon, C. H., "Numerical analysis on the thermal characteristics of photovoltaic module with ambient temperature variation", Solar Energy Materials and Solar Cells, 95, pp. 404–407, 2011.

[19] Salmi, T., Bouzguenda, M., Gastli, A. & Masmoudi, A., "Matlab/Simulink Based Modelling of Solar Photovoltaic Cell", International Journal of Renewable Energy Research, 2(2), pp. 214-218, 2012.

[20] Kane, A. & Verma, V., "Performance Enhancement of Building Integrated Photovoltaic Module using Thermoelectric Cooling", International Journal of Renewable Energy Research, 3(3), pp. 321-324, 2013.

[21] Vergura, S., Acciani, G. & Falcone, O., "3-D PV-cell Model by means of FEM", *IEEE*-ICCEP, pp. 35-40, Capri, Italy, 9-11 June 2009.

[22] Usama Siddiqui, M., Arif, A.F.M., Kelley, L. & Dubowsky, S., "Three-dimensional thermal modeling of a photovoltaic module under varying conditions", Solar Energy, 86, pp. 2620–2631, 2012.

[23] Jicheng Zhou, Qiang Yi, Yunyun Wang & Zhibin Ye., "Temperature distribution of photovoltaic module based on finite element simulation", Solar Energy, 111, pp. 97-103, 2015.

[24] Lee, Y. & Tay, A.A.O., "Finite element thermal analysis of a solar photovoltaic module", Energy Proceeding, 15, pp. 413–420, 2012.

[25] Dhatt, D., Touzot, G., Lefrançois, L., Méthode des éléments finis, Paris : Hermes Science, 2005.

[26] Boulfaf, N., Chaoufi, J., Ghafiri, A. & Elorf, A., "Thermal Study of Hybrid Photovoltaic Thermal (PV-T) Solar Air Collector Using Finite Element Method", International Journal of Renewable Energy Research, 6(1), pp. 171-182, 2016.

Nomenclature

α	absorptivity
τ	transmissivity
λ	thermal conductivity
T^*	virtual temperature field
c	specific heat
σ	Stefan-Boltzmann's constant
$\{T\}$	nodal vector temperature
v	air speed
T_a	ambient temperature
h	convective heat transfer coefficient
V	domain
$\vec{n}$	outward unit normal at a considered point
$[A^e]$	transfer matrix (for passing from element to layer)
$[P]$	transfer matrix (for passing from layer to global structure)
ρ	material density
ε	emissivity
G	incident solar intensity
β	packing factor of solar cell
η_{ref}	efficiency at standard test condition
a	ambient
g	glass
c	solar cell
ted	tedlar
ref	reference
e	elementary
EVA	ethyl vinyl acrelate
E	thickness
S	area